NANO LETTERS

Letter

pubs.acs.org/NanoLett

MoS_2 Nanosheet Phototransistors with Thickness-Modulated Optical Energy Gap

Hee Sung Lee,[†] Sung-Wook Min,[†] Youn-Gyung Chang,[†] Min Kyu Park,[‡] Taewook Nam,[§] Hyungjun Kim,[§] Jae Hoon Kim,[†] Sunmin Ryu,[‡] and Seongil Im*[,†]

[†]Institute of Physics and Applied Physics and [§]School of Electrical and Electronic Engineering, Yonsei University, Seoul 120-749, Korea

[‡]Department of Applied Chemistry, Kyung Hee University, Yongin, Gyeonggi 446-701, Korea

Supporting Information

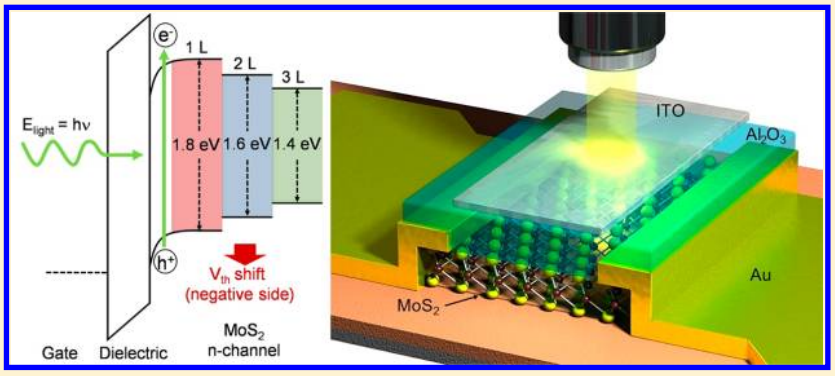

ABSTRACT: We report on the fabrication of top-gate phototransistors based on a few-layered MoS_2 nanosheet with a transparent gate electrode. Our devices with triple MoS_2 layers exhibited excellent photodetection capabilities for red light, while those with single- and double-layers turned out to be quite useful for green light detection. The varied functionalities are attributed to energy gap modulation by the number of MoS_2 layers. The photoelectric probing on working transistors with the nanosheets demonstrates that single-layer MoS_2 has a significant energy bandgap of 1.8 eV, while those of double- and triple-layer MoS_2 reduce to 1.65 and 1.35 eV, respectively.

KEYWORDS: *MoS_2, phototransistor, photoresponse, energy gap*

Graphene and related two-dimensional (2D) nanosheet materials have been studied with much attention in view of their promising applications to future nanoelectronics.[1,2] Graphene exhibits a high carrier mobility (μ) over 100 000 $cm^2/V{\cdot}s$, but it also reveals considerable limitations in regards to real device applications, due to an intrinsic difficulty caused by its small bandgap (E_g).[3−5] In fact, the E_g of graphene turned out to be less than 200 meV;[6,7] so, graphene could hardly be used for switching circuits or photodetecting devices which need clearly defined on-and-off states. Molybdenum disulfide (MoS_2) layers very recently appeared as an alternative nanosheet material that may overcome the drawbacks of graphene, even if prepared by the same exfoliation technique.[8−11] Bulk MoS_2 is known to have an indirect bandgap of ~1.2 eV, but the few angstrom-thin single-layered MoS_2 has recently been reported to exhibit a direct bandgap of 1.8 eV.[11−16] In fact, the E_g change of MoS_2 with thickness has previously been forecasted by theoretical estimations.[17−19] According to recent reports, a few-layered MoS_2 displayed light absorption and luminescence capabilities, enabling a photo-transistor operation.[16,20] However, the phototransistors with MoS_2 channel reported so far showed a very low mobility of ~0.3 $cm^2/V{\cdot}s$, basically using thick thermally oxidized SiO_2 layers (on p^{+2}-Si wafer) as the back gate dielectric, in which way any practical applications are hardly probable.[20] For practical phototransistors, superior mobility and subthreshold swing are mandatory along with compatibility to circuit integration. To satisfy those properties in MoS_2-based phototransistors, the transparent and patterned top-gate approaches are mostly required, including high-k dielectric deposition on the MoS_2 channel.[11]

In this Letter, we demonstrate for the first time a transparent top-gate phototransistor with single-, double-, and triple-layer MoS_2 nanosheets, which was respectively analyzed by photo-electric probing as equipped with a patterned transparent gate electrode on a top of 50 nm-thin oxide dielectric.[21] Our device with triple-layer MoS_2 showed some loss of low-dimensional electric properties but instead exhibited good photodetection capabilities for red and green lights. In contrast, those with single- and double-layer MoS_2 exhibited such good nanodevice

Received: April 20, 2012
Revised: May 31, 2012
Published: June 11, 2012

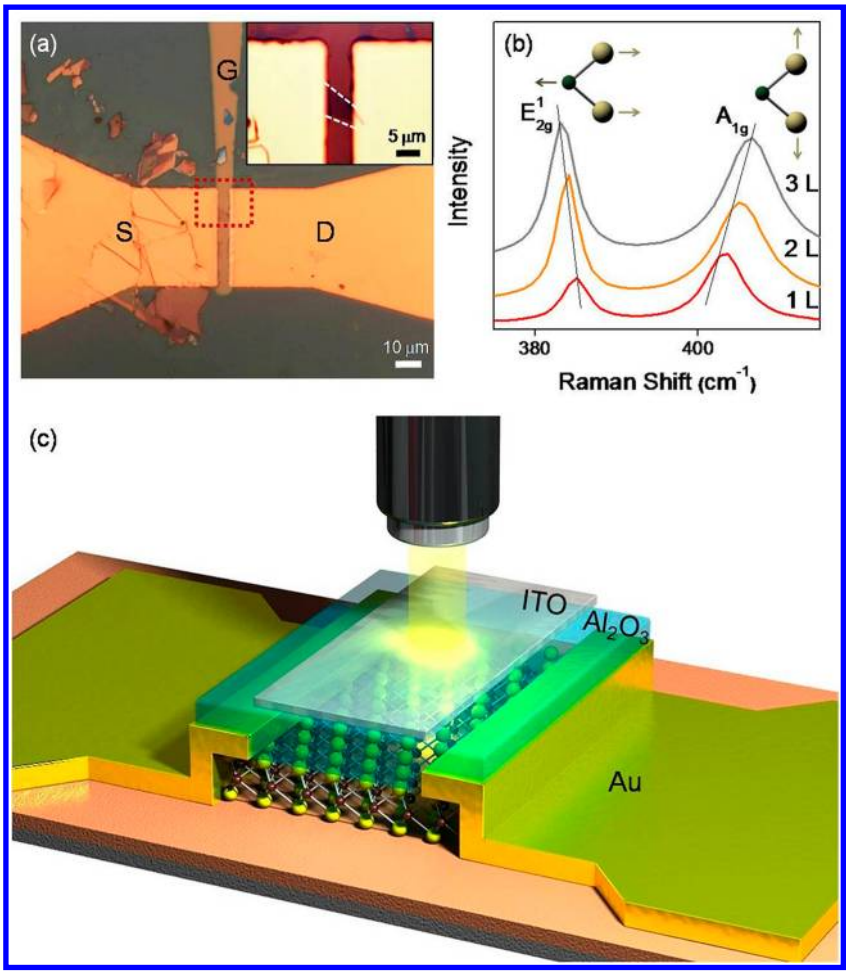

Figure 1. (a) Optical image of the single-layer MoS_2-based top-gate transistor. The inset photograph shows a zoomed image of Au S/D electrodes, ITO top-gate, and exfoliated MoS_2. (b) Raman spectra of single-, double-, and triple-layer MoS_2. The inset image shows atomic displacements of the two Raman-active modes: E^1_{2g} and A_{1g}. (c) Schematic 3D view of single-layer transistor with hexagonal structure MoS_2 nanosheet, 50 nm-thick Al_2O_3 dielectric, and ITO top-gate under monochromatic light.

properties as high mobilities and unsaturated output current, while they appeared to be useful for green and ultraviolet light detection. According to our photoelectric probing results from the working nanosheet transistors, single-layer MoS_2 has a significant energy bandgap of 1.82 eV, while those with double- and triple-layer MoS_2 showed reduced values of 1.65 and 1.35 eV, respectively. We thus regard that the electrical and photoelectric properties of the nanosheet can be promisingly modulated by the thickness of the sheet, since the total number of layers controls the mobility and the optical bandgap as well.

A surface-cleaned 285 nm-thick SiO_2/p^{+2}-Si wafer was chosen as the substrate for our n-type MoS_2 nanosheet transistor with Au source/drain (S/D) electrodes, since 285 nm was reported as an optimal thickness to identify few-layer dichalcogenide.[22] Indeed, each exfoliated MoS_2 flake showed a distinctive optical contrast with thinner flakes exhibiting a lower optical density, which enabled fast screening of few-layered flakes under an optical microscope. Even though other exfoliated flakes exist around our single-layer MoS_2, as shown in the optical microscopy image of Figure 1a for transistor top view, our nanosheet transistors operated well. Our MoS_2 nanosheet flakes were ~10 μm on one side, so that a long 5 μm channel was available for our device (W/L ratio was ~1). (Fabrication and measurement details are introduced in Supporting Information and Figure S1a–d). In Figure 1b, Raman spectra obtained from three samples were respectively assigned to single-, double-, and triple-layered MoS_2 flakes spanning ~5 × 5 μm^2. As shown by the previous report, the frequency difference between E^1_{2g} and A_{1g}, the two prominent Raman-active modes of 2H-MoS_2 crystals, decreases stepwise with the decreasing number of layers.[23] The interpeak separation or frequency difference for the thinnest flake in Figure 1b is 18.0 ± 1.0 cm^{-1}, which is in excellent agreement with that for single-layer MoS_2.[23,24] (The thickness of monolayer MoS_2 was measured by previous researchers to be ~0.65 nm.)[11] Confirming the layer number of exfoliated flakes by Raman spectra, we respectively selected MoS_2 nanosheets as the channel of our phototransistors. Figure 1c illustrates the three-dimensional (3D) scheme of our transparent top-gate phototransistor with MoS_2 nanosheet and atomic-layer-deposited (ALD) 50 nm-thin Al_2O_3.

Figure 2a–c displays the drain current–gate voltage (I_D–V_G) transfer characteristics of our top-gate nanosheet transistors. Their on/off current ratio was higher than 10^7 for the single- and double-layer MoS_2 nanosheet transistors and was ~10^6 for the triple-layer transistor. The linear mobility μ_{lin} was respectively estimated to be 80, 27, and 10 cm^2/V·s as maximum values for single-, double, and triple-layer nanosheets, when it was plotted as a function of V_G (respective insets) based on the following equations: $g_m(V_G) = dI_D/dV_G$

dx.doi.org/10.1021/nl301485q | Nano Lett. 2012, 12, 3695–3700

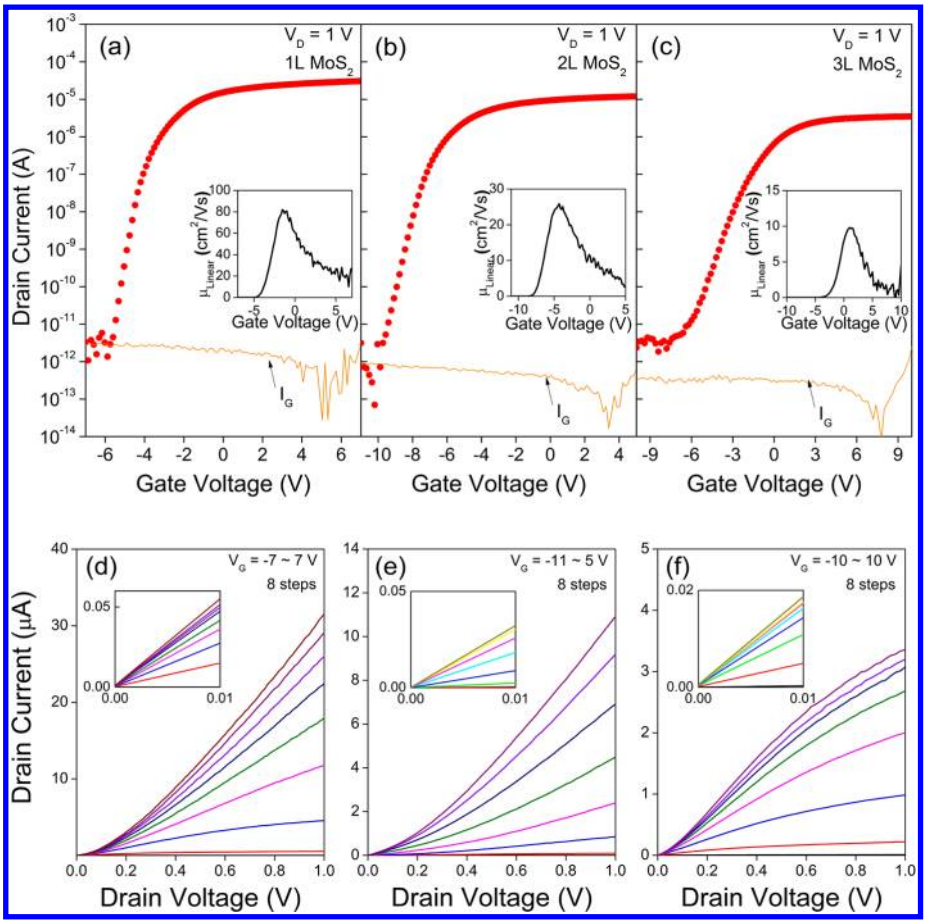

Figure 2. The transfer curves of top-gate transistors with (a) single-, (b) double-, and (c) triple-layer MoS_2. Measurements were performed at V_D = 1 V, and I_G means gate leakage current. Respective inset curves show V_G-dependent linear mobility plots. I_D−V_D output curves of (d) single-, (e) double-, and (f) triple-layer MoS_2-based transistors. Respective insets show an almost ohmic contact behavior between Au S/D and MoS_2 nanosheet.

(transconductance) and $\mu_{lin} = (g_m/C_{ox}V_D)*(L/W)$, where C_{ox} and V_D are dielectric capacitance and drain voltage, respectively. The subthreshold swing (SS) of our single-layer MoS_2 transistor was ∼300 mV/dec, while it increases (degrades) with the total layer number. The μ_{lin} and SS values of our top-gate transistor with single-layer nanosheet trail the world record values of previously reported transistors[11] but are much superior to the values from double- and triple-layer MoS_2 transistors. According to the output (drain current−drain voltage; I_D−V_D) characteristics of our nanosheet transistors (Figure 2d−f), the source/drain contacts of our nanosheet transistors are almost ohmic with respect to Au regardless of their thickness (see the respective insets). However, the linear I_D behavior was only maintained with single- and double-layered MoS_2 transistors, while the relatively thick triple-layer transistor showed slightly saturated I_D curves, probably due to the increase of thickness-direction scattering and some loss of dielectric screening, both of which cause the nanosheet to deviate from its low dimensional properties, such as high mobility and linear I_D characteristics.[25−27]

Figure 3a−c displays the photoinduced transfer curves of our transparent top-gate nanosheet transistors, on which monochromatic red (λ = 680 nm; photon energy ε ∼1.82 eV), green (λ = 550 nm), and ultraviolet (UV; λ = 365 nm) lights were applied. The average illumination intensity was controlled to be ∼0.1 mW/cm^2 for all the wavelength photons probing on our devices. The single-layer MoS_2 transistor hardly responds to red light, while the other two nanosheet transistors show quite good photoresponses to the red. Green and UV lights were well detected by all the nanosheet transistors regardless of their total layer number. Since the red light was not efficiently detected by the single-layer MoS_2 transistor, causing little threshold voltage (V_{th}) shift or photocurrent, we regard that the single-layer MoS_2 has an optical energy gap higher than or equivalent to 1.82 eV, and thus we performed a photoelectric probing experiment on our nanosheet transistors using more than 50 serial monochromatic photon beams ranging from low to high, 1.2 to 2.0 eV, respectively, energies, to measure their optical energy gap.[21] Based on the series of photoinduced transfer characteristics of our nanosheet transistors (acquired at a drain voltage of V_D = 1 V; see Figure S2, Supporting Information for the 50 phototransfer curves from our three MoS_2 transistors), we measured the series of photoinduced threshold voltage shift $\Delta V_{th}(\varepsilon)$ and plotted $\Delta Q_{eff}(\varepsilon)$ [= $C_{ox}\cdot\Delta V_{th}(\varepsilon)$] with respect to the photon energy, ε (see Figure S3, Supporting Information, for the photoelectric probing experiment details). Regarding any small trap density at the interface between MoS_2 and Al_2O_3 dielectric since our MoS_2 layer surface has few dangling bonds in tact,[11] we can expect that a considerable ΔV_{th} is only observed with the photon energy higher than the optical energy gaps of respective nanosheets, as illustrated with their schematic band diagrams within a ITO/Al_2O_3/MoS_2 structure in Figure 3d. According to the plots of Figure 3e, the approximate optical energy gaps are found to be 1.35, 1.65, and 1.82 eV for triple-,

dx.doi.org/10.1021/nl301485q | Nano Lett. 2012, 12, 3695−3700

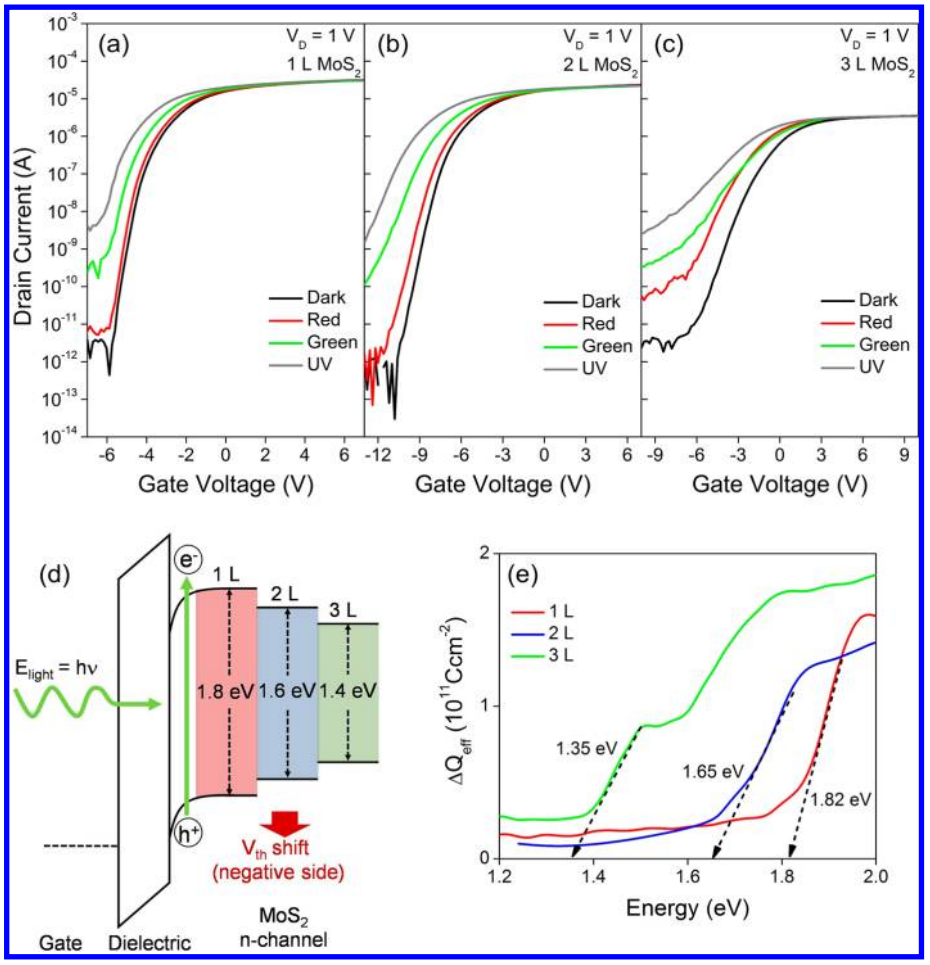

Figure 3. The photoinduced transfer curves of respective top-gate transistors with (a) single-, (b) double-, and (c) triple-layer MoS_2 under monochromatic red, green, and UV lights. (d) The schematic band diagrams of ITO (gate)/Al_2O_3 (dielectric)/single (1 L)-, double (2 L)-, triple (3 L)-layer MoS_2 (n-channel) under the light (E_{light} = hν) illustrate the photoelectric effects for band gap measurements. (e) Photon energy-dependent ΔQ_{eff} plots indicate the approximate optical energy gaps to be 1.35, 1.65, and 1.82 eV for triple-, double-, and single-layer MoS_2 nanosheets, respectively.

double-, and single-layer MoS_2 nanosheets, respectively, while little ΔV_{th} is observed below 1.35 eV, indicating small interface trap density. It means that the band gaps are thickness modulated, and comparable results were also recently reported from the photoconductivity measurement of the single- and double-layer MoS_2 nanosheets.[16] We now understand why the red light detection was so marginal in our single-layer nanosheet transistor, where the largest slope in the plot of Figure 3e is also noticed at the band-to-band transition onset (1.82 eV) as an indicator of direct gap character.[16]

Such photoresponse was again observed in a dynamic way over a 5 s interval for light-switching with the top-gate transistors. According to the time domain plot of Figure 4a−c, the red light response increases with the total layer number; the triple-layer MoS_2 nanosheet transistor appeared to show the largest dynamic photogain under the red light switching. These photocurrent dynamics were measured under respectively different off-state V_G conditions for the three MoS_2 transistors, based on the transfer curves in Figure 3a−c. On the one hand, the green detection appears quite the same regardless of the layer number, while the average response time (average of 80% rise and fall) of single-, double-, and triple-layer MoS_2 phototransistors was respectively observed to be 1.5, 1, and ∼0.3 s. In falling behavior, an approximate exponential decay was observed. As a representative for voltage dynamics, the double-layer MoS_2 nanosheet transistor among the three devices was selected, to form a photoinverter with a serially connected 22 MΩ resistor (inset of Figure 4d). According to the voltage transfer curves (VTCs) of Figure 4d, the voltage shift by green light is as large as 0.7 V, while the shift by red is minimal to be only less than 0.1 V. (Its electrical VTC curves are also shown in Figure S4, Supporting Information.) In Figure 4e, the voltage dynamics of the photoinverter was displayed; under the conditions of 1 V supply voltage (V_{DD}) and 2 s on-and-off light intervals, the photoinduced voltage gain of 0.26 V was achieved by green light, while the red resulted in only 0.06 V. The signal voltage for the red light would increase with the triple-layer nanosheet transistor due to its reduced optical energy gap. We display similar photo-VTC curves and voltage dynamics of another photoinverter with single-layer MoS_2 in Figure S5, Supporting Information, where we dynamically switch the device using the UV and green lights. These photoinverter operations are applicable to more practical devices, such as photosense amplifier or photogating logic devices, providing a connected device with a certain voltage signals that are caused by photocurrent, while a classical inverter provides logic functions by electrical gating (Figure S4, Supporting Information).[28]

dx.doi.org/10.1021/nl301485q | *Nano Lett.* 2012, 12, 3695−3700

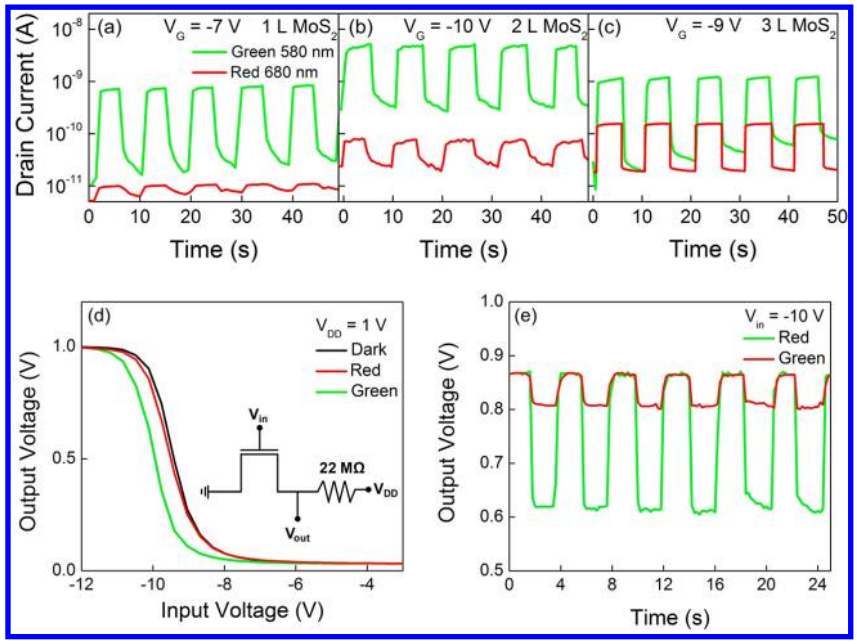

Figure 4. Respective photocurrent dynamics of (a) single-, (b) double-, and (c) triple-layer MoS_2-based top-gate transistors under monochromatic red and green lights. (d) Dark and photoinduced VTC curves of our photoinverter composed of serially connected 22 MΩ resistor and double-layer MoS_2 transistor (see the inset for the circuit). (e) Voltage dynamics of the resistive-type photoinverter under monochromatic red and green lights.

In summary, we have fabricated the top-gate phototransistors based on single-, double-, and triple-layer MoS_2 nanosheet. Our devices with triple-layer exhibited improved photodetection capabilities for red light, while the others with single- and double-layers were more useful for green light detection. Such differences were attributed to the thickness-modulated optical gap of nanosheets. According to our photoelectric probing technique on working transistors with the nanosheets, single-layer MoS_2 has a significant energy bandgap of 1.82 eV, while those of double- and triple-layer MoS_2 showed 1.65 and 1.35 eV, respectively.

■ ASSOCIATED CONTENT

Supporting Information

Specific experimental procedures, optical microscope images of double- and triple-layer MoS_2-based devices, specific method of photoelectric probing system, voltage transfer characteristics of double-layer MoS_2-based inverter, and photoinduced voltage curves of single-layer MoS_2 transistor. This material is available free of charge via the Internet at http://pubs.acs.org.

■ AUTHOR INFORMATION

Corresponding Author

*E-mail: semicon@yonsei.ac.kr. Telephone: 82-2-2123-2842.

Notes

The authors declare no competing financial interest.

■ ACKNOWLEDGMENTS

The authors acknowledge the financial support from NRF (NRL program, no. 2012-0000126), BK21 Project. H.S.L. acknowledges the tuition support from the LOTTE fellowship. J.H.K. acknowledges the financial support from NRF (program no. 2011-0000990). S.R. acknowledges the financial support from NRF (program no. 2011-0031629).

■ REFERENCES

(1) Geim, A. K. *Science* **2009**, *324*, 1530−1534.
(2) Novoselov, K. S.; Jiang, D.; Schedin, F.; Booth, T. J.; Khotkevich, V. V.; Morozov, S. V.; Gein, A. K. *Proc. Natl. Acad. Sci. U.S.A.* **2005**, *102*, 10451−10453.
(3) Novoselov, K. S.; Geim, A. K.; Morozov, S. V.; Jiang, D.; Chang, T.; Grigorieva, I. V.; Firsov, A. A. *Science* **2004**, *306*, 666−669.
(4) Berger, C.; Song, Z.; Li, T.; Li, X.; Ogbazghi, A. Y.; Feng, R.; Dai, Z.; Marchenkov, A. N.; Conrad, E. H.; First, P. N.; Heer, W. A. *J. Phys. Chem. B* **2004**, *108*, 19912−19916.
(5) Bolotin, K. I.; Sikes, K. J.; Jiang, Z.; Klima, M.; Fudengerg, G.; Hone, J.; Kim, P.; Stormer, H. L. *Solid State Commun.* **2008**, *146*, 351−355.
(6) Han, M. Y.; Ozyilmaz, B.; Zhang, Y.; Kim, P. *Phys. Rev. Lett.* **2007**, *98*, 206805.
(7) Sols, F.; Guinea, F.; Castro Neto, H. *Phys. Rev. Lett.* **2007**, *99*, 166803.
(8) Coleman, J. N.; Lotya, M.; O'Neill, A.; Bergin, S. D.; King, P. J.; Khan, U.; Young, K.; Gaucher, A.; De, S.; Smith, R. J.; Shvets, I. V.; Arora, S. K.; Stanton, G.; Kim, H. Y.; Lee, K.; Kim, G. T.; Duesberg, G. S.; Hallam, T.; Boland, J. J.; Wang, J. J.; Donegan, J. F.; Grunlan, J. C.; Moriarty, G.; Shmeliov, A.; Nicholls, R. J.; Perkins, J. M.; Grieveson, E. M.; Theuwissen, K.; McComb, D. W.; Nellist, P. D.; Nicolosi, V. *Science* **2011**, *331*, 568−571.
(9) Wu, H.; Yang, R.; Song, B.; Han, Q.; Li, J.; Chang, Y.; Fang, Y.; Tenne, R.; Wang, C. *ACS Nano* **2011**, *5*, 1276−1281.
(10) Bertolazzi, S.; Brivio, J.; Kis, A. *ACS Nano* **2011**, *5*, 9703−9709.
(11) Radisavljevic, B.; Radenovic, A.; Brivio, J.; Giacometti, V.; Kis, A. *Nat. Nanotechnol.* **2011**, *6*, 147−150.
(12) Eda, G.; Yamaguchi, H.; Voiry, D.; Fujita, T.; Chen, M.; Chhowalla, M. *Nano Lett.* **2011**, *11*, 5111−5116.
(13) Splendiani, A.; Sun, L.; Chang, Y.; Li, Y.; Kim, J.; Chim, C. Y.; Galli, G.; Wang, F. *Nano Lett.* **2010**, *10*, 1271−1275.
(14) Ramasubramaniam, A. *Phys. Rev. B* **2010**, *4*, 4677−4682.
(15) Han, S. W.; Kwon, H.; Kim, S. K.; Ryu, S.; Yun, W. S.; Kim, D. H.; Hwang, J. H.; Kang, J. S.; Baik, J.; Shin, H. J.; Hong, S. C. *Phys. Rev. B* **2011**, *84*, 045409.
(16) Mak, K. F.; Lee, C.; Hone, J.; Shan, J.; Heinz, T. F. *Phys. Rev. Lett.* **2010**, *105*, 136805.
(17) Kuc, A.; Zubouche, N.; Heine, T. *Phys. Rev. B* **2011**, *83*, 245213.

(18) Li, T.; Galli, G. *J. Phys. Chem.* **2007**, *111*, 16192−16196.
(19) Lebegue, S.; Eriksson, O. *Phys. Rev. B* **2009**, *79*, 115409.
(20) Yin, Z.; Li, H.; Li, H.; Jiang, L.; Shi, Y.; Sun, Y.; Lu, G.; Chang, Q.; Chen, X.; Chang, H. *ACS Nano* **2012**, *6*, 74−80.
(21) Lee, K.; Oh, M. S.; Mun, S. J.; Lee, K.; Ha, T. W.; Kim, J. H.; Ko, S. H. K.; Hwang, C. S.; Lee, B. H.; Sung, M. M.; Im, S. *Adv. Mater.* **2010**, *22*, 3260−3265.
(22) Benameur, M. M.; Radisavljevic, B.; Heron, J. S.; Sahoo, S.; Berger, H.; Kis, A. *Nanotechnology* **2011**, *22*, 125706.
(23) Lee, C.; Yan, H.; Brus, L. E.; Heinz, T. F.; Hone, J.; Ryu, S. *ACS Nano* **2010**, *4*, 2695−2700.
(24) Ghatak, S.; Pal, A. N.; Ghosh, A. *ACS Nano* **2011**, *5*, 7707−7712.
(25) Jena, D.; Konar, A. *Phys. Rev. Lett.* **2007**, *98*, 136805.
(26) Cudazzo, P.; Tokatly, I. V.; Rubio, A. *Phys. Rev. B* **2011**, *84*, 085406.
(27) Molina-Sanchez, A.; Wirtz, L. *Phys. Rev. B* **2011**, *84*, 155413.
(28) Radisavljevic, B.; Whitwick, B. B.; Kis, A. *ACS Nano* **2011**, *5*, 9934−9938.